

Creation of Imprinted Textured Substrates to Evaluate their Erosion - Corrosion Resistance

Adil Keku Gazder

Department of Mechanical Engineering

Shiv Nadar University

December 2021

The content, materials, and any other elements associated with this project, including but not limited to text, graphics, images, code, and design, are the intellectual property of the author and are protected by copyright law. Any commercial use or distribution of the materials without prior written consent from the author is strictly prohibited.

1. Acknowledgements

Though the pandemic brought on several difficulties along the way, our research work was able to proceed uninterrupted thanks to the constant support and guidance of Dr. Harpreet Grewal at every step of the way. I would not have learnt as much as I did without sir's mentorship and counsel. I would also like to express my gratitude towards Amit Sharma, Mayank Garg, Arunesh Kumar and Gopinath Perumal who have supported me extensively during the course of my work. Lastly, I would like to thank the Department of Mechanical Engineering, Shiv Nadar University for this opportunity to contribute to this field which I am constantly fascinated by.

Table Of Contents

S. No.	Content	Page No.
1.	Acknowledgements	3
2.	List of Figures	5
3.	List of Abbreviations	7
4.	Abstract	8
5.	Introduction	9
6.	Materials and Methods	14
6.1	Materials Used	14
6.2	Synthesis	14
6.3	Surface Characterization	15
6.4	Experimental Details	18
7.	Results and Discussion	20
7.1	Slurry Erosion Testing	20
7.2	Corrosion Testing	22
8.	Conclusion	23
9.	References	24

2. List of Figures

Figure Number	Description
<i>Fig. 01</i>	Comparative view of the images showing textures visible on the (a) Galapagos Sharks, (b) Hammerhead Sharks, (c) Bull Sharks and (d) Snake Skin
<i>Fig. 02</i>	Schematic Diagram of the interaction at the interfaces between the grooves and the flow.
<i>Fig. 03</i>	FESEM Images of the Stainless Steel Conventionally Manufactured, imprinted at 125 Kg/cm^2 (Left) and the Stainless Steel Conventionally Manufactured, imprinted at 175 Kg/cm^2 (Right).
<i>Fig. 04</i>	FESEM Images of the Stainless Steel Additively Manufactured, imprinted at 125 Kg/cm^2 (Left) and the Stainless Steel Additively Manufactured, imprinted at 175 Kg/cm^2 (Right).

Fig. 05

FESEM Images of the major grooves as visible on the Stainless Steel Conventionally Manufactured, imprinted at 175 Kg/cm² (Left) and the Stainless Steel Additively Manufactured, imprinted at 175 Kg/cm² (Right).

Fig. 06

3D Profilometry Image of the Stainless Steel Conventionally Manufactured, imprinted at 125 Kg/cm² (Top Left) imprinted at 175 Kg/cm² (Middle Left) and the Stainless Steel Additively Manufactured, imprinted at 175 Kg/cm² (Bottom Left). The corresponding depth profiles are also attached.

Fig. 07

Schematic diagram showing the Slurry Erosion setup.

Fig. 08

Graphical comparison between Conventionally Manufactured and Additively Manufactured samples under different impingement angles (30° and 90°) when subject to Slurry Erosion Testing (Top Left), Slurry Erosion Corrosion Testing (Top Right) and the textured samples performance under Slurry Erosion Testing (Bottom Left).

Fig. 09

Graphical comparison between Conventionally Manufactured and Additively Manufactured as-cast and imprinted samples under Corrosion Testing

3. List of Abbreviations

Abbreviations	Description	Units
<i>AM</i>	Additive Manufacturing	-
<i>C</i>	Corrosion Rate	mpy
<i>D</i>	Diameter of the Impinging Particle	m
<i>DI</i>	De-Ionized	-
<i>E</i>	Erosion Loss	mm ³ /hr
<i>eCorr</i>	Corrosion Potential	mV
<i>ECW</i>	Erosion Corrosion Wear	-
<i>FESEM</i>	Field Emission Scanning Electron Microscope	-
<i>H_v</i>	Vickers Hardness of the Substrate	N/mm ²
<i>iCorr</i>	Corrosion Current Density	A/cm ²
<i>N_f</i>	Number of Impacts	-
<i>OCP</i>	Open Circuit Potential	-
<i>p</i>	Density of the Impinging Particle	g/cm ³
<i>SCE</i>	Saturated Calomel Electrode	-
<i>SS</i>	Stainless Steel	-
<i>V</i>	Velocity of the Impinging Particle	m/sec

4. Abstract

Humans have always tried to optimize the surfaces created to try and achieve a better tribological performance such as Higher Wear Resistance and a Lower Coefficient of Friction leading the list. This research project aims to implement biomimicry to understand how nature has uniquely designed surfaces such as Shark Skins or Reptile Scales which tend to decrease drag and increase the wear resistance of the surface, using textures, patterns and designs. We try to mimic these textures on a micro-scale to understand if and how they tend to affect the erosion and corrosion resistance of the substrate. Our study also offers a comparative overview between the different types of structures created under plastic deformation. Lastly, with Additive Manufacturing techniques being more extensively applied in the industry, we try and also compare the wear performance of additively vs conventionally manufactured textured substrates, understanding to what extent the substrate properties can affect erosion - corrosion rates. The samples were tested using a Slurry Erosion Setup and a Corrosion Setup, all while mimicking the operating conditions of Stainless Steel used under marine conditions.

5. Introduction

Erosion and wear still stand as one of the biggest challenges that any industry faces. Erosion is characterized as the disturbance of a materials surface coating caused due to particle interaction (usually at a high velocity) and Corrosion is the removal of the protective surface coating of a material due to an electrochemical interaction. Erosion and Corrosion mechanisms differ broadly and more often than not, we find both erosion and corrosion acting together, we term this as Erosion - Corrosion Wear (ECW). [10] The ECW observed can be attributed to a mechanochemical effect which depends on several factors such as Surface Structure and Composition, Chemical Properties of the Electrolyte, Operating Conditions etc, all for which we control and try to understand over the course of this project. The real problem arises when we know that there are multiple erosion - corrosion mechanisms which play out in different situations, depending on whether the material is brittle or ductile, flat or textured, the velocity and impact angle of the impinging particles, corrosivity of the media etc. [11] Erosion in ductile materials for example occurs by considerable plastic flow and large plastic strain occurs before fracture, however with brittle materials, erosion occurs with crack formation propagation, leading to material loss by chipping. This could mean that with brittle materials exposed to highly corrosive media, due to the increase in exposed surface area, we may find a very high corrosion rate observed. With erosion mechanisms, the two main mechanisms we hypothesized would play out on the surface of the material was the Ductile Erosion Mechanism and the Two Phase Gas Flow Mechanism. The ductile erosion mechanism was modelled similar to Sheldon and Kanhere which says that the material removal per particle can be given by

$$W = \frac{D^3 V^3 p^{3/2}}{H_v^{3/2}}$$

Where,

W is the Material Removal per particle

D is the impinging Particle Diameter

V is the Particle Velocity

ρ is the Particle Density

H_v is the Vickers Hardness of the material

They were also able to prove that the mechanism for material removal from a single particle and multiple particle erosions are the same, only a few additional factors such as particle impact within the stream, particle fragmentation, particle embedding and rebounding of particles. The impinging particle's size, shape, velocity, angle of impingement, temperature and surface properties of the substrate all influence the ductile material erosion, most of which have an exponential dependence on by the erosion rate. Randomized rebounding of particles after impact, irrespective of impact angle, is in fact what makes the Two Phase Gas Flow erosion mechanism much more effective. The energy loss during a single particle impact was also modelled by Hutchings where he states that the volume loss per impact after N_f impacts can be modelled as

$$\text{Volume Loss per impact after } N_f \text{ impacts} = \frac{\alpha m v^2}{2 P N_f}$$

and erosion loss 'E' defined as the mass lost per unit mass of impinging particles can be given by

$$\text{Erosion Loss (E)} = \frac{\alpha \rho v^2}{2 P N_f}$$

Where,

α is the fraction of volume of indentation which is plastically deformed

ρ is the density of the substrate

M is the mass of the impinging particle

v is the impact velocity of the impinging particle

P is the constant pressure of resistance to indentation by substrate

Energy balance during impact showed that at least 90% of the initial kinetic energy of the particle is dissipated in plastic deformation in the target, meaning that the rebounding particle has less than 10% of the initial kinetic energy it had, all lost during the first elastic collision

with the target surface. We note here firstly in these equations all elastic effects have been ignored, and that if in this mechanism we can find a way to increase N_f , i.e. the number of impacts on the surface which happens, the erosion loss E will decrease and the particle will exponentially lose the initial kinetic energy it had available for plastic deformation, with each additional impact it has with the target surface. Based on previous studies, patterns observed in nature such as the scales on the body of a shark or the skin of a scorpion or a snake, each species has adapted itself to the harsh environment they live in. For sharks, where the surfaces are subjected to high flow velocities and wall shear stress, the scales are oriented in such a way that there is a significant reduction in drag observed, similar to scorpion skin [1].

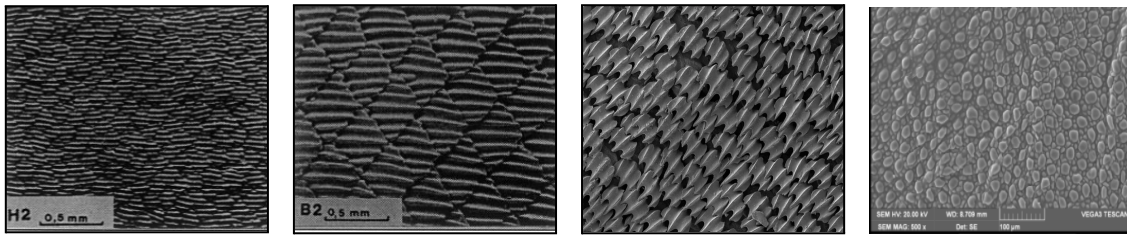


Fig. 01: Comparative view of the images showing textures visible on the (a) Galapagos Sharks, (b) Hammerhead Sharks, (c) Bull Sharks and (d) Snake Skin.

The idea of texturing and creating microgrooves on our substrate via imprinting was to try and increase N_f during the erosion mechanism for this reason. With the additional impacts generated and disturbance in flow direction, due to the rotating flow of the media in the microgrooves, an ‘air cushion’ effect is also observed where the trapped air and fluid flow between the textured surface and the flow can absorb some of the striking particle’s energy and hence the net energy during impact is reduced further, which is what enhances the erosion resistance majorly. This is what is termed as the Two Phase Gas Flow. Previous studies show that almost a 7.3% decrease in turbulent shear stress was observed with a textured surface, compared to a smooth reference plate. The importance of texture geometry has also been emphasized because that is what dictates the impact angle of the impinging particle onto the surface. [6]

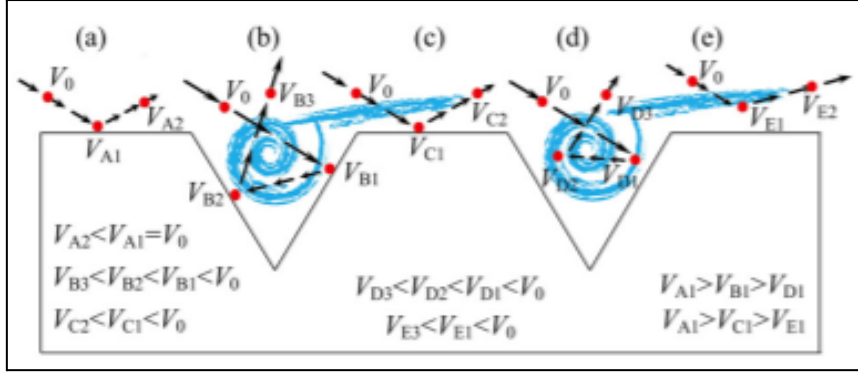


Fig. 02: Schematic Diagram of the interaction at the interfaces between the grooves and the flow [6].

Apart from our approach to patterning, we had also considered other solutions which may lead to a reduction in the material erosion rate, mainly the use of Surface Coatings. During our literature review itself we understood that coatings alone may not be as effective, as with the initial erosion leading to a loss of protective film and/or the erosive media chemically interacting with the coating, we will see an increase in the ECW observed. This initial erosion attack entirely depends on the impact velocity and turbulence of the flow and nature of the contaminant particles. Due to the speed of the media and its own corrosive properties, it can eat through any protective layers before going on to damage the metal itself. The flow generated damage may also create additional local pressure surges and high shear stresses on the surface, which may also be aggravated due to cavitation and the movement of gritty particles and hot gas vapours. Hence surface coatings alone would not suffice for this [13].

Now understanding the need for texturing in our study, we had several options for texturing our samples including Subtractive Manufacturing (Laser Patterning/Micromachining), Additive Manufacturing (3D Printing), Imprinting etc. With some of these methods however the material may become susceptible to micro/nano scale surface damages, subsurface crack formation and microstructural changes. This is why we had decided to go with an imprinting technique for the surface patterning, taking advantage of its low-cost, efficiency and ease of implementation and setup. Additionally during texturing via imprinting, there is no need for an abrasive media or a coolant, with high levels of automation possible. From the production perspective, different manufacturing processes can be used which can affect the intrinsic

mechanical properties of the substrate, targeting a reduction in erosion - corrosion wear from an early stage itself. Apart from our material selection, we explored not only how conventionally manufactured textured samples will perform but also offer a comparative overview with how additively manufactured textured samples will perform under similar testing conditions. Additive Manufacturing techniques hold a major advantage over Subtractive Manufacturing techniques from a cost perspective (material wastages), production time, amount of human intervention needed, versatility in design etc. We hypothesize that due to the layered design of the substrate and the thermal gradient generated during manufacturing within the bulk of the material, the textured substrate may behave differently when compared to a conventionally manufactured substrate [3].

This research work comparatively evaluates the erosion and corrosion resistance of conventionally and additively manufactured imprinted textured substrates under marine conditions.

6. Materials and Methods

6.1. Materials Used

Our chosen substrate material is Stainless Steel SS316L (Density: 7.80 g/cm³), a Austenitic Steel alloy with Chromium (16-18%), Nickel (10-14%), Molybdenum (2%), Manganese (2%) and the rest trace elements, chosen due to its potential applications in various industries, specifically the marine industry, due to its intrinsic strength and corrosion resistant nature makes it highly durable. The high corrosion resistant nature of Stainless Steel can be attributed to its high Chromium content, which reacts on exposure to atmosphere forming Chromium Oxide (Cr₂O₃), a passive oxide layer which prevents further rusting of the substrate. The addition of Molybdenum also increases corrosion resistance by resisting local pitting and corrosive attack by the chloride ions and also increases its strength at higher temperatures. 316 Grade Stainless Steel is the most effective in very acidic environments. SS316L has been chosen instead of SS316 as the low Carbon content in the substrate means lesser deleterious carbide precipitation and it can be used extensively for medical applications [12]. The additive samples were manufactured using metal powder bed fusion with a laser power of 200 W, exposure time 75 us, beam diameter 70 um and a striped scan pattern.

6.2. Synthesis

Our substrate preparation involved first machining commercially available Stainless Steel SS316L to dimensions of 10 x 10 x 5 mm sample, further polished using Abrasive Polishing sheets of different grades (80, 220, 400, 600, 800, 1000, 1500, 2000) (Manufacturer: 3M). We then performed ultrasonication on our samples present in a Deionized (DI) water bath to get rid of any dust and debris for 10 mins at 35°C. The samples were then textured via imprinting. Using a wire mesh mould (Stainless Steel 25 Mesh Size, Plain Weave type) for patterning, the mesh was placed on top of the polished sample in a Hydraulic Press (Manufacturer: Bainmount H). Samples were subject to different imprinting pressures (125

Kg/cm^2 and 175 Kg/cm^2), for a comparative overview, for a loading time of 10 mins. All processes were carried out under highly sterile conditions and Acetone (99.9%) was used primarily as our cleaning agent during processing. All testing and measurements were done under ambient conditions ($24 \pm 2^\circ\text{C}$ and relative humidity of around 35%) unless mentioned otherwise.

6.3. Surface Characterization

The surface morphology of the untextured and textured samples were characterized and compared using a field emission scanning electron microscope (FESEM). The mapped surfaces are shown and compared in Fig. 03 and Fig. 04. We used a scan size of at least $1.1 \times 1.8 \text{ mm}^2$ for each scan having scanned a minimum of three random locations for each sample and average values were reported.

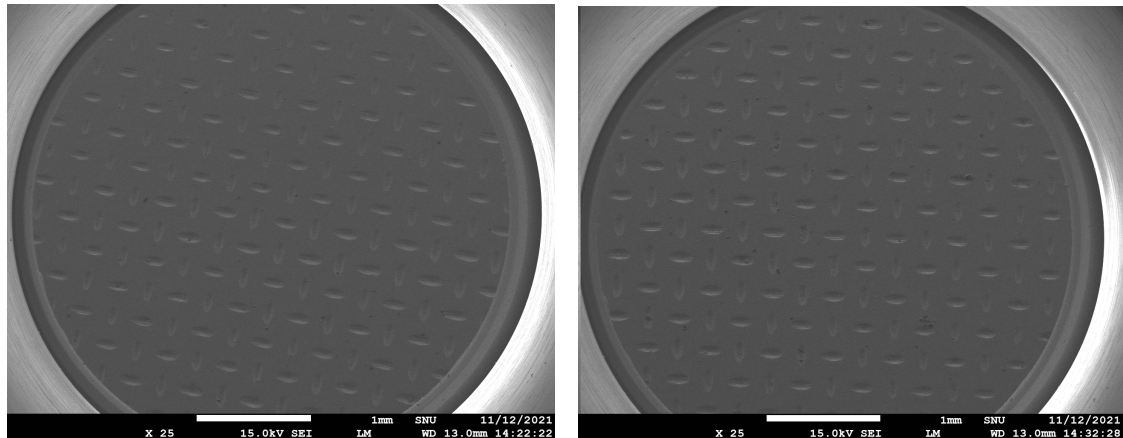


Fig. 03: FESEM Images of the Stainless Steel Conventionally Manufactured, imprinted at 125 Kg/cm^2 (Left) and the Stainless Steel Conventionally Manufactured, imprinted at 175 Kg/cm^2 (Right).

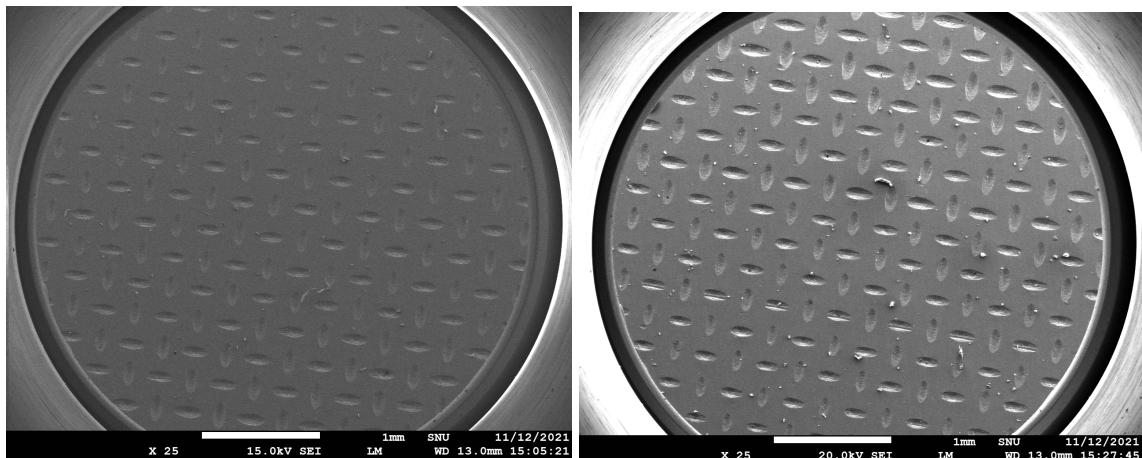


Fig. 04: FESEM Images of the Stainless Steel Additively Manufactured, imprinted at 125 Kg/cm² (Left) and the Stainless Steel Additively Manufactured, imprinted at 175 Kg/cm² (Right).

Additionally we were able to capture the perpendicular orientation of the individual imprints visible on the grid pattern on the substrate with the FESEM. A comparative view of the imprints on the conventionally and additively manufactured samples are visible in Fig 05. We note that the additively manufactured sample has a much more defined imprint boundary. The disparity in the crack formation on the imprint boundary proves vital with the erosion corrosion mechanism later on.

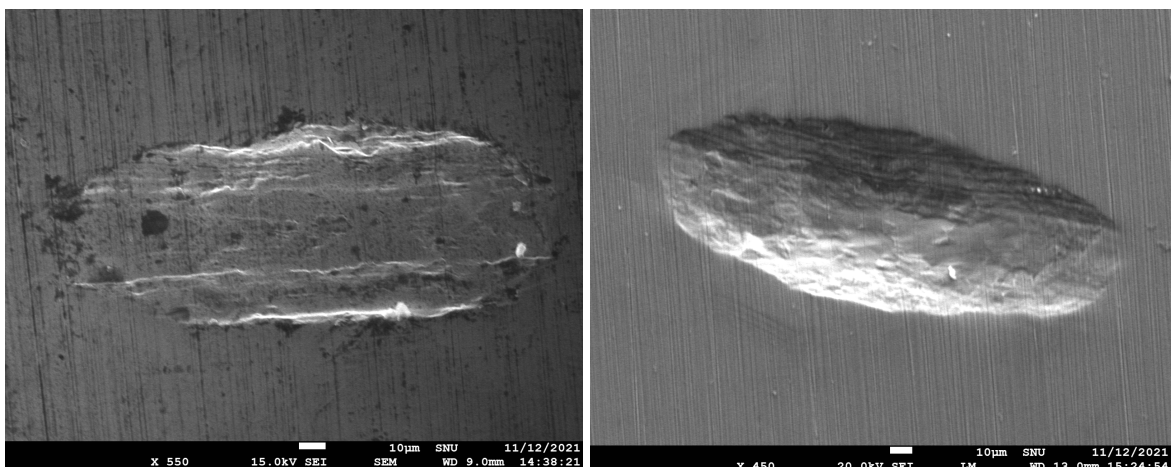


Fig. 05: FESEM Images of the major grooves as visible on the Stainless Steel Conventionally Manufactured, imprinted at 175 Kg/cm² (Left) and the Stainless Steel Additively Manufactured, imprinted at 175 Kg/cm² (Right).

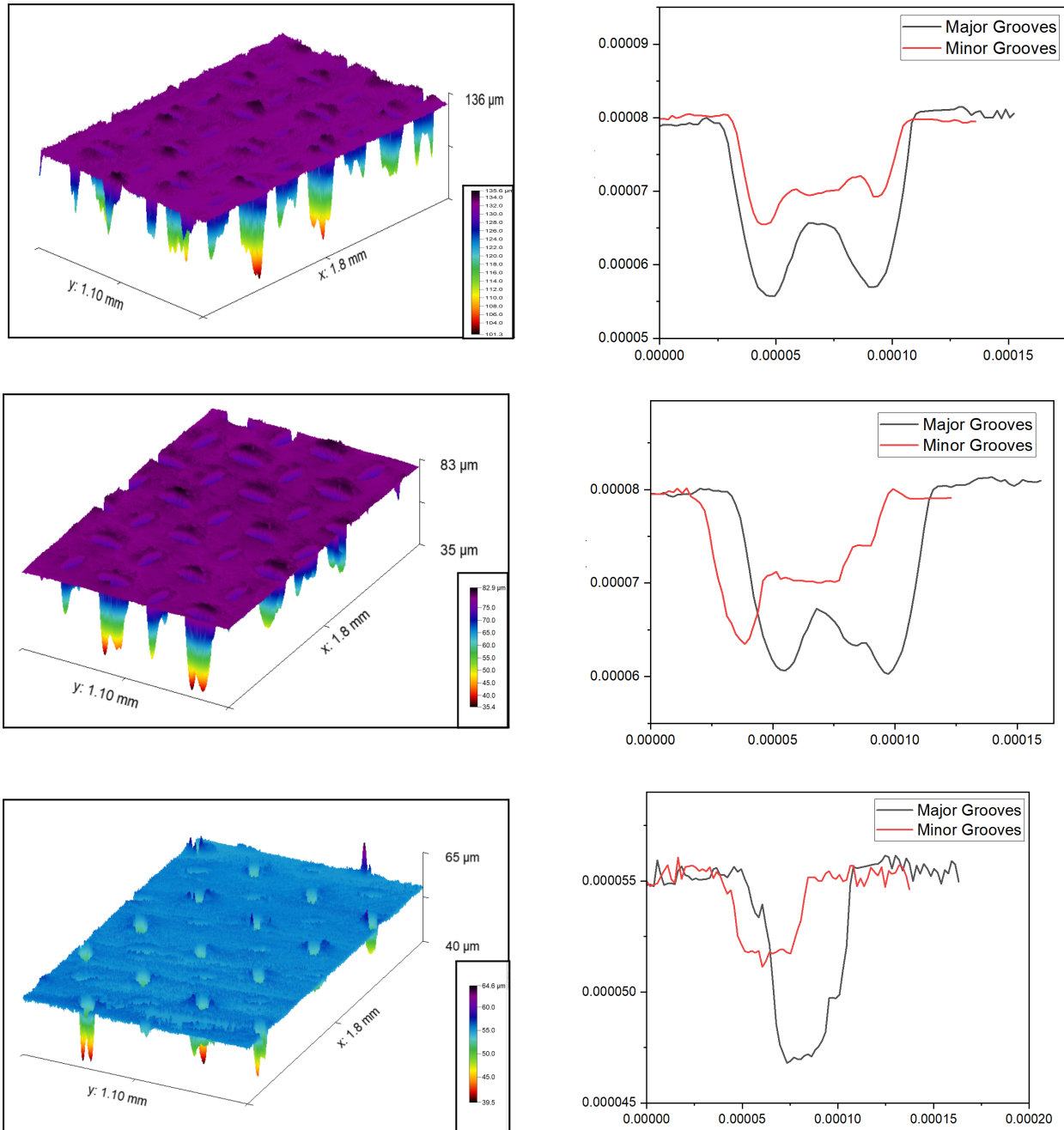


Fig. 06: 3D Profilometry Image of the Stainless Steel Conventionally Manufactured, imprinted at 125 Kg/cm² (Top Left) imprinted at 175 Kg/cm² (Middle Left) and the Stainless Steel Additively Manufactured, imprinted at 175 Kg/cm² (Bottom Left). The corresponding depth profiles are also attached. All values shown are in meters unless mentioned otherwise.

The 3D profilometry and depth profiles for the textured samples were obtained. The grooves visible after imprinting on all samples were classified as major and minor grooves, depending on their shape and depth. We notice the pattern had alternating major and minor grooves, oriented mutually perpendicular to each other, as evident in Fig. 04. The depth profiles for the textured samples were compared. The major groove depth ranged between 11 - 30 um and the minor groove depth ranged between 5 - 19 um. Something unique we noticed was that with the samples, in some cases the depth of the imprint was not proportional to the pressure applied during imprinting, and this was especially evident with the additively manufactured samples.

6.4. Experimental Details

The Slurry Erosion apparatus was set up as shown in the schematic below. The sample was first subject to ultrasonication in a DI water bath for 10 mins at 35°C. The sample was then weighed thrice before being mounted, making a 90° angle with the impinging jet. The slurry jet contained 12.5g of sand (particle diameter 75-150 um) dissolved in 2.5L of water and was made to impact with a pressure of 3 Bar. To study the erosion corrosion resistance, an additional 87.5g of NaCl was added to the slurry media. The slurry was constantly mixed at 900 - 1100 rpm to ensure consistency in the impacting slurry jet, and the setup was completed using a diaphragm pump. The slurry jet was impacted on the sample for 2 hours, following which ultrasonication was performed again and then the slurry was weighed to calculate mass loss and erosion rate.

The calculations for the slurry erosion and slurry erosion corrosion rates are as follows,

$$\text{Mass Loss} = \text{Final Mass} - \text{Initial Mass} \quad (\text{in g})$$

$$\text{Volume Loss} = \frac{\text{Mass Loss} * 1000}{\text{Substrate Density}} \quad (\text{in mm}^3/\text{hr})$$

$$\text{Erosion Rate} = \frac{\text{Volume Loss}}{2} \quad (\text{in mm}^3/\text{hr})$$

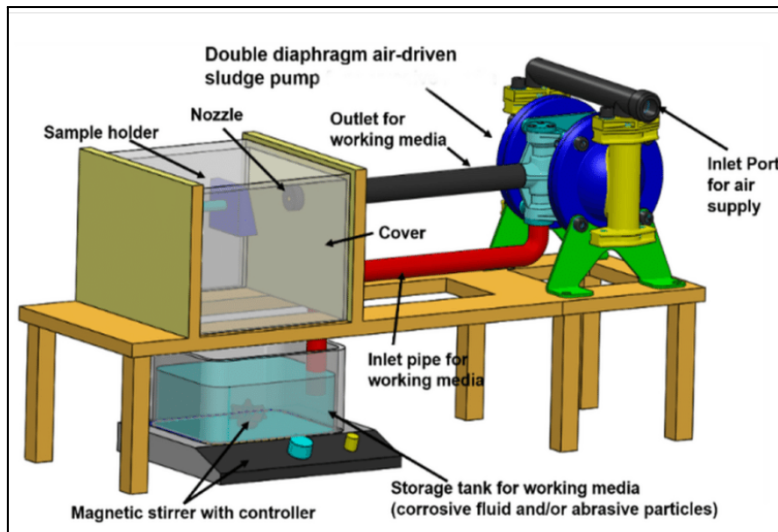


Fig. 07: Schematic diagram showing the Slurry Erosion setup [8].

For the corrosion tests, the substrates were subject to an Electrochemical Corrosion test, using a Three Electrode Setup. The Working Electrode is connected to the sample (which acts as the Anode), a Graphite Counter Electrode was used (which acts as the Cathode) and a Saturated Calomel Electrode (SCE) as the Reference Electrode. The Open Circuit Potential (OCP) was first performed followed by a Potentiodynamic Polarization Scan to check the corrosion performance of the sample. The electrolyte used was a 3.5% NaCl + DI Water solution. The Corrosion Potential (eCorr Value), Corrosion Current Density (iCorr Value) and the Corrosion Rates were obtained after the Tafel Fitting.

7. Results and Discussions

7.1. Slurry Erosion Testing

The comparative results of Slurry Erosion and Slurry Erosion Corrosion tests performed on untextured conventional vs additively manufactured samples are shown in Fig. 08. We note that in the case of Slurry Erosion Testing, the Conventionally Manufactured Samples tends to outperform the Additively Manufactured Samples with a lower erosion rate of $0.47 \text{ mm}^3/\text{hr}$ when the impingement angle is 30° , however, when subject to a 90° impingement angle, the Additively Manufactured Sample shows a lower erosion rate. Even in the case of the Slurry Erosion Corrosion testing, under different impingement angles, we observe similar results, with the Additively Manufactured Sample showing better results at 30° impingement, and Conventionally Manufactured Sample showing better results at 90° impingement.

When we compare the performance of the Untextured and Textured Conventionally Manufactured Samples when subject to Slurry Erosion Testing, we note that the Textured Sample has a much lower erosion rate ($0.303 \text{ mm}^3/\text{hr}$) as compared to the Untextured Sample, indicating that a different erosion mechanism occurs with textured samples, as hypothesized. Between the Untextured and Textured samples, we notice almost a 47.7% decrease in the erosion rate, and if it can be attributed to the Two Phase Mechanism, it can be extensively applied across domains.

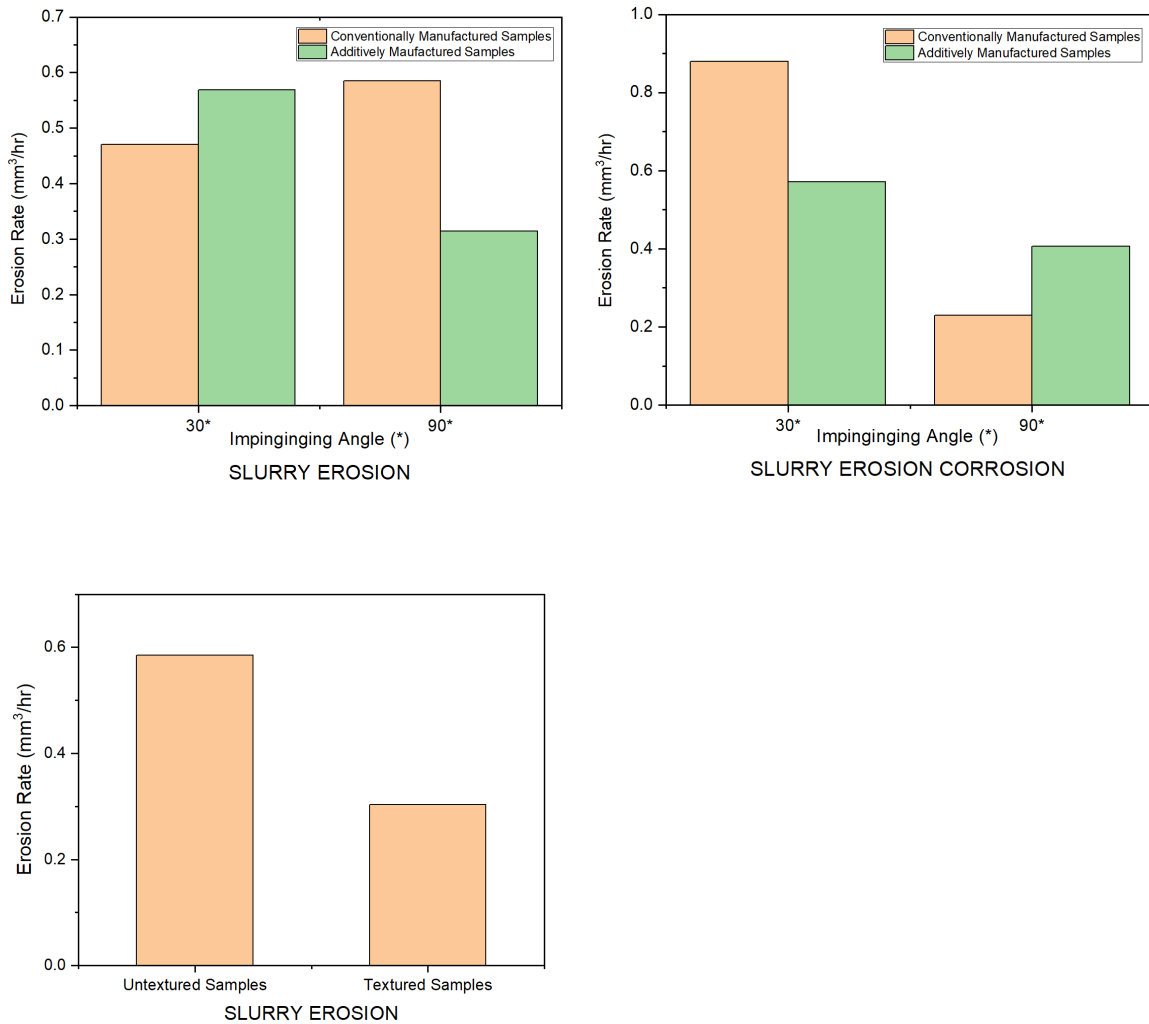


Fig. 08: Graphical comparison between Conventionally Manufactured and Additively Manufactured samples under different impingement angles (30° and 90°) when subject to Slurry Erosion Testing (Top Left), Slurry Erosion Corrosion Testing (Top Right) and the textured samples performance under Slurry Erosion Testing (Bottom Left).

7.2. Corrosion Testing

The comparative results after corrosion testing on the different samples have been plotted in Fig. 09 as shown. We also define 'Imprint Pressure' as the pressure applied on the sample during imprinting. If we compare the Untextured (As-Cast) and Textured samples, as we tested samples with increasing Imprint Pressure, we see an increase in the Corrosion Rate observed. This can directly be attributed to the increase in the exposed surface area on the sample, allowing the surface to corrode much more extensively than the As-Cast sample. This trend is observed both with Conventionally Manufactured and Additively Manufactured samples when compared.

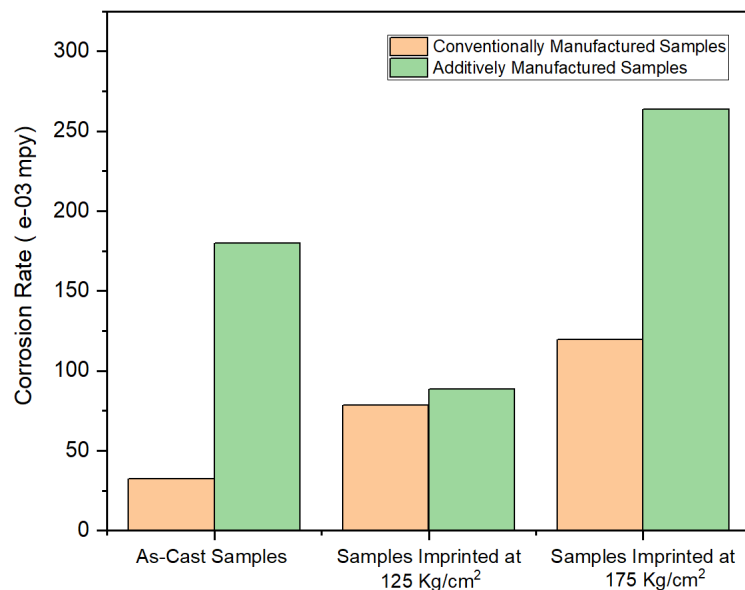


Fig. 09: Graphical comparison between Conventionally Manufactured and Additively Manufactured as-cast and imprinted samples under Corrosion Testing.

8. Conclusion

Our work began with an extensive literature review on textured surfaces, their durability and their applications across domains. We then went on to prepare our Conventionally and Additively Manufactured Stainless Steel SS316L samples by first polishing and then imprinting the samples using a wire mesh mould in a hydraulic press at different pressures (125 kg/cm^2 and 175 kg/cm^2) to get a comparative overview of their performance. FESEM, 3D Profilometry and Optical Microscopy images were collected before the samples were tested for their erosion resistance, corrosion resistance and their erosion-corrosion resistance under marine conditions. Our Slurry Erosion results showed a significant decrease in the erosion rate of the textured sample compared to the untextured sample and we did find additively manufactured samples performing much poorly than conventionally manufactured samples. With the corrosion test results, we were conclusively able to say that due to an increase in the exposed surface area of the sample, the corrosion rates of textured samples were much higher than that of untextured samples.

The future scope of this research work could include understanding how effective and durable a combination of texturing and then coating the substrate surface would be when exposed to similar conditions. We are also keen on exploring how different surface textures could affect not only the tribological but also the mechanical properties of the substrate.

9. References

- [1] D. W. Bechert, M. Bruise, W. Hage. “Experiments with three-dimensional riblets as an idealized model of shark skin”, Experiments in Fluids, 2000.
- [2] Radha, Lim, Saifullah, Kulkarni. “Metal hierarchical patterning by direct nanoimprint lithography”. Scientific Reports, 2013.
- [3] Sinmazcelik, Fidan, Urgun. “Effects of 3D printed surface texture on erosion wear”, Tribology International, 2019.
- [4] Arumugaprabu, Ko, Kumaran, Kurniawan, Uthayakumar. “A brief review on importance of surface texturing in materials to improve the tribological performance”. Rev.Advanced Material Science, 2018.
- [5] Jung, Yang, Jung, Kim. “Anti-erosion mechanism of a grooved surface against impact of particle-laden flow”. Wear, 2018.
- [6] Han, Yin, Jiang, Niu, Ren. “Erosion-Resistant surfaces inspired by Tamarisk”. Journal of Bionic Engineering, 2013.
- [7] Zhao, Tang, Liu, Zhang. “Finite element analysis of anti-erosion characteristics of material with patterned surface impacted by particles”. Powder Technology, 2018.
- [8] R.B. Nair, H.S. Arora, S. Mukherjee, S. Singh, H. Singh, H.S. Grewal. “Exceptionally High Cavitation Erosion and Corrosion Resistance of a High Entropy Alloy”. Ultrasonics Sonochemistry, 2017,
- [9] Xu, Zhang, Zhou, Gao, Wang, Wang, Huang. “Flow accelerated corrosion and erosion-corrosion behavior of marine carbon steel in natural seawater”. Materials Degradation, 2021.
- [10] Sohn, Yang, Lee, Park. “Sensing solutions for assessing and monitoring of nuclear power plants (NPPs)”. Sensor Technologies for Civil Infrastructures.

[11] Ramesh Padavala."Failure Mechanisms in impact erosion of ductile materials". Graduate Theses, Dissertations and Problem Reports. 2004.

[12] <https://www.thoughtco.com/type-316-and-316l-stainless-steel-2340262>

[13] <https://www.corrosionpedia.com/2/1868/corrosion-prevention/metallic-and-ceramic-coatings/erosion-corrosion-coatings-and-other-preventive-measures>